# Experimental conditions for suppressing Edge Localised Modes by magnetic perturbations in ASDEX Upgrade

W Suttrop[1], A Kirk[2], V Bobkov[1], M Cavedon[1], M Dunne[1], N Leuthold[1], R M McDermott[1], H Meyer[2], R Nazikian[3], C Paz-Soldan[4], D A Ryan[2], E Viezzer[1,5], M Willensdorfer[1], the ASDEX Upgrade[1] and MST1[2] Teams

[1]Max Planck Institute for Plasma Physics, Boltzmannstrasse 2, 85748 Garching, Germany
[2]CCFE Culham Science Centre, Abingdon, Oxon, OX14 3DB, UK
[3]Princeton Plasma Physics Laboratory, PO Box 451, Princeton, NJ 08543-0451, USA
[4]General Atomics, PO Box 85608, San Diego, CA 92186-5608, USA
[5]Dept. of Atomic, Molecular and Nuclear Physics, University of Seville, 41012 Seville, Spain

The Edge Localised Mode (ELM) instability presents a significant challenge for the power handling in a next step fusion device, and mitigation of ELMs is a clear requirement for ITER [1]. One of the most promising techniques, the complete suppression of ELMs by resonant magnetic perturbations (MP), has been pioneered in DIII-D (see, e.g. the overview in Ref. [2]) and subsequently been reproduced, among other tokamaks, in ASDEX Upgrade (AUG) [3, 4] in plasmas with moderately elevated triangularity. In a current journal article [5], the empirical criteria to access ELM suppression in ASDEX Upgrade are investigated. They can be summarised as follows: 1. The poloidal spectrum of the MP must be aligned for best plasma response from weakly stable kink-modes, which amplify the perturbation [6], 2. The plasma edge density must be below a critical value, $3.3 \times 10^{19}$ m$^{-3}$. It is not clear to date how this condition can be expressed in dimensionless (and therefore extrapolatable) parameters, 3. The pedestal pressure must be kept sufficiently low to avoid the return of (small) ELMs. 4. The edge safety factor $q_{95}$ lies within a certain window, $q_{95} = 3.57 - 3.95$ as has been identified so far. 5. Within the range of plasma rotation encountered so far, no apparent threshold of plasma rotation for ELM suppression is found. This includes cases with large cross field electron flow in the entire pedestal region. Here, we report additional recent experimental observations that pertain to (a) the role of plasma triangularity and (b) the role of resonant rational surfaces for accessing ELM suppression.

The plasma scenario employed here is similar to that used in Refs. [3] and [5]. Plasmas are heated with 6 MW neutral beam (NB) power (fully co-$I_p$ injected) and up to 2.4 MW electron cyclotron heating power (ECRH) at 140 GHz, absorbed centrally at the third harmonic (X3) at the toroidal field $B_t = -1.83$ T. Central heating is successful to maintain peaked temperature profiles and prevent accumulation of heavy impurities from the all-metal wall of AUG in the absence of a strong gas puff. The plasma current is $I_p = 0.885$ MA or $I_p = 0.9$ MA for an edge safety factor about $q_{95} = 3.8$ and 3.74, respectively. The AUG in-vessel saddle coils are used here exclusively to produce $n = 2$ MPs with a differential phase $\Delta\Phi = 90^\circ$ between upper and lower coil rings, which is found optimal to reach ELM suppression in the above plasma scenario [5].

Figure 1 shows time traces of discharge 34835, which starts up like the pulses described in Refs [3] and [5]. ELM suppression is reached at about $t = 3.0$ s, followed by a slow ramp of the ELM suppression plasma shape with upper triangularity $\delta_u \sim 0.2$ towards a shape with triangularity of $\delta_u \sim 0.05$ at $t = 5.0$ s. This final shape is similar to the configuration in which ELMs were mitigated but not suppressed [3, 4].

[1]See A Kallenbach et al, Nucl Fus **57** (2017) 102015
[2]See H Meyer et al, Nucl Fus **57** (2017) 102014

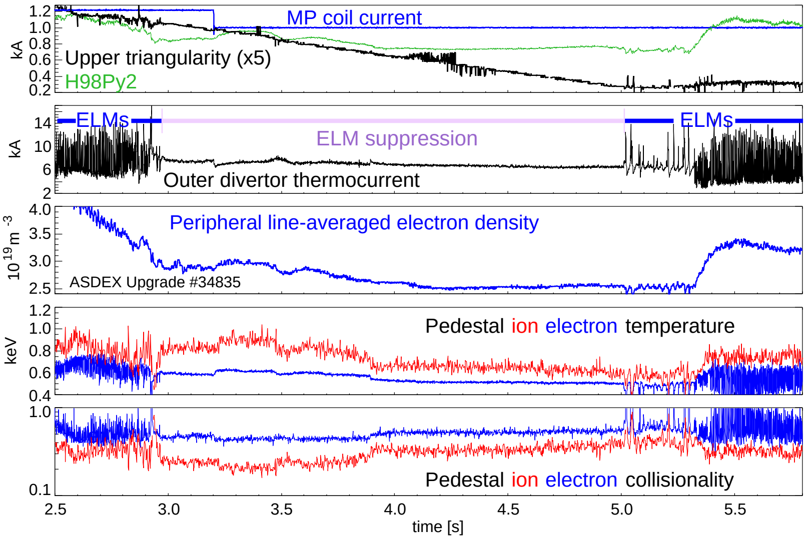


Figure 1: Discharge 34835, testing ELM suppression during a ramp of the upper triangularity.

ELM suppression, as seen by the absence of ELM spikes in the outer divertor thermocurrent (second panel) is maintained until the end of the shape ramp. The end of ELM suppression is marked with a phase of infrequent ELMs at $t = 5.0$ s, before frequent ELMs take over after $t = 5.32$ s. In this intermediate phase ($t = 5.0 - 5.32$ s), the baseline of the divertor thermocurrent is still elevated and similar to that of the ELM suppression phase, indicating that there is significant inter-ELM transport. The inter-ELM losses slow down the pedestal recovery after each ELM and are thus the likely reason for the observed reduced ELM frequency. The transport mechanism that governs the low plasma density and the stationarity during ELM suppression is obviously not precluding the occurrence of ELMs. At $t = 3.2$ s, the MP coil current is stepped down from 1.2 kA to 1.0 kA, which results in a temporary increase of peripheral plasma density $n_{e,p}$, pedestal ion and electron temperatures ($T_{i,\mathrm{ped}}$, $T_{e,\mathrm{ped}}$) and hence pedestal pressure. The confinement factor is also increasing. In the course of the plasma shape ramp, $n_{e,p}$ as well as $T_{i,\mathrm{ped}}$, $T_{e,\mathrm{ped}}$ are decreasing, most strongly between $t = 3.3$ s and 4.0 s, when $\delta_u = 0.16 - 0.12$. Clearly, the pedestal pressure is governed by both plasma shaping and the MP strength which are main parameters to optimise confinement of ELM suppression plasmas.

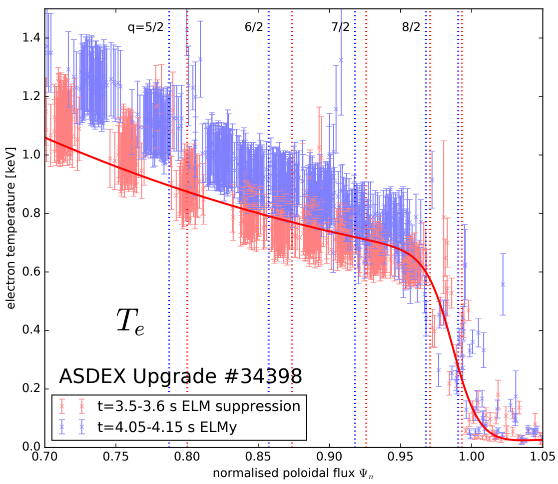


Figure 2: Edge temperature profiles in ELMy H-mode and ELM suppression.

We now consider the role of resonant rational surfaces for ELM suppression, i.e. surfaces where $q = m/n$ where $m$ is the poloidal mode number of a non-vanishing spectral component of the MP. Resonant surfaces are special because of the possibility of a resistive (tearing) response to the applied MP which can cause a modification of the magnetic topology and lead to braking torque and enhanced radial transport along the magnetic field around islands or in an ergodised volume. In a model proposed in Refs. [7], profile flattening at a resonant surface near the top of the H-mode barrier can prevent the edge gradient region from expanding towards the core plasma and potentially keep the plasma edge stable against an ELM crash if the resonant surface is located at a suitable position near the top of the gradient region. Such a model implies a sensitivity of ELM suppression to the value of the edge safety factor $q_{95}$ which is indeed observed in DIII-D [8]. Also in ASDEX Upgrade, the loss of ELM suppression can be provoked by small variations of $q_{95}$. Figure 2 shows edge electron temperature ($T_e$) profiles for one case of Ref. [5], discharge 34398, taken during two time intervals, $t = 3.5-3.6$ ($q_{95} = 3.88-3.94$, ELM suppression) and $t = 4.05-4.15$ ($q_{95} = 4.01-4.02$, ELMing). The $q = 8/2$ surface is near the top of the gradient region in the suppressed case, es expected in the model. The radial shift that corresponds to the $q$ change which causes the transition to ELMing H-mode is very small.

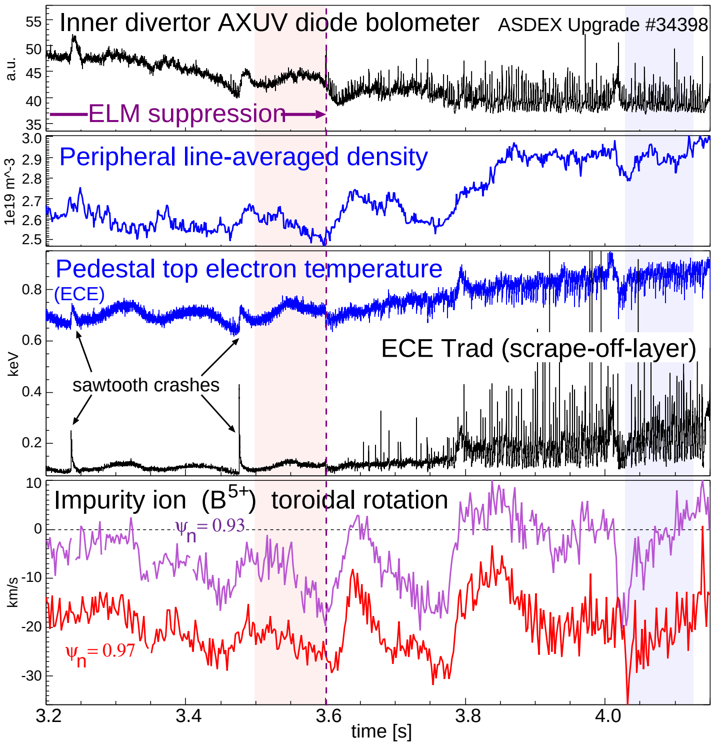


Figure 3: Time traces during backtransition from ELM suppression to ELMing H-mode.

Times traces of this discharge around the backtransition are shown in Fig. 3. The coloured areas correspond to the time intervals of the $T_e$ profiles in Fig. 2. ELM activity is well diagnosed by several measurements, notably inner divertor radiation measured with diode bolometers (top panel) and spikes in the electron cyclotron emission (ECE) in a channel with cold ECE resonance in the scrape-off layer (third panel). These spikes are believed to be partly due to downshifted emission from energetic electrons in the confined plasma caused by reconnection events in sawtooth and ELM crashes. The transition from ELM suppressed to ELMing at $t =$ 3.6 s is sharp and occurs within a few ms or less. After the transition, the inner divertor bolometer signal drops and $T_e$ and $n_e$ begin to rise, indicating a loss of the transport mechanism that maintains ELM suppression. Soon after (from $t = 3.65$ s), small ELMs appear which grow as the pedestal pressure increases. The bottom panel shows the toroidal impurity ($B^{5+}$) rotation velocity $v_{tor}$, taken at $\Psi_n = 0.93$ (pedestal top, at $q = 7/2$) and $\Psi_n = 0.97$ (gradient region, at $q = 8/2$). A sharp change of the rate-of-change of $v_{tor}$ is detected at the backtransition, $t = 3.6$ s near $q = 7/2$. At $q = 8/2$, $v_{tor}$ lags behind by a few ms. If the backtransition is caused by a torque change at a rational surface then this observation indicates that the torque acts more likely at $q = 7/2$ rather than at $q = 8/2$.

In ASDEX Upgrade, repetitive transitions between ELM suppression and ELMing H-mode can be observed, although rarely. Figure 4 shows time traces with three such cycles. During ELM suppression, the plasma density and impurity ion rotation at the pedestal and in the core drop, while in the ELMing phases they recover. It is interesting to note that in the gradient region, $\Psi_n = 0.95$, the $v_{tor}$ reverses into the direction opposite to the plasma current only during ELMy phases. This reversal occurs very quickly at the times of the backtransition. We may speculate that the nature of the dominant torque input onto the plasma by the MP changes. Strong braking towards zero rotation is consistent with a resonant plasma response to the MP, while the reversal of the rotation direction may be indicative of approaching intrinsic rotation associated with neoclassical toroidal viscosity (NTV). NTV torque is usually much weaker than resonant torque and would be noted only in the absence of the latter. The repetitive transitions are reminiscent of limit cycle oscillations such as dithering H-mode transitions. However, the state variable governing the transitions is unknown to date.

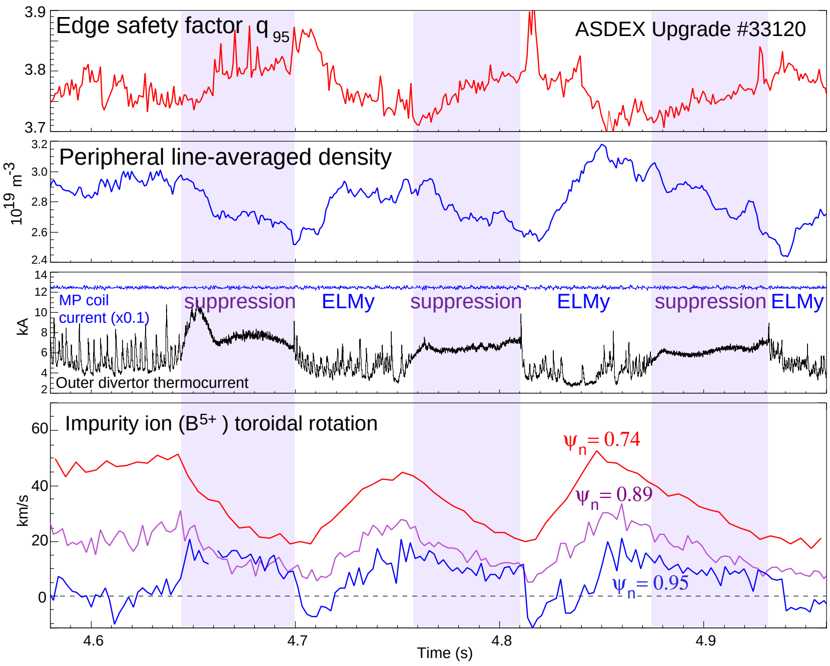


Figure 4: A discharge with repeated transition between ELMy and ELM-suppressed H-mode. The $B^{5+}$ impurity ion rotation changes sign in early ELMy phases.

We observe a change of $q_{95}$ (top panel of Fig. 4) which is probably caused by current profile changes due to the transitions and hence implies that the (edge) current diffusion time scale governs the time between transitions. However, the maximum value of $q_{95} \approx 3.85$, reached at the backtransition, is not near a bound of the $n = 2$ suppression window found in Ref. [5].

In summary, we can compare our observations in ASDEX Upgrade with the model of Refs. [7]. The existence of $q_{95}$ access windows for ELM suppression, the position of a resonant surface at $q = 8/2$ near the gradient top, and the braking torque during ELM suppression support the existence of a resonant response during ELM suppression. However, the resonant response can be shielded by cross-field flows. In ASDEX Upgrade, surprising insensitivity of ELM suppression access to flow variations is found, including cases with strong electron rotation $\omega_{e,\perp}$ everywhere in the edge region [5], which is predicted in two-fluid MHD to be the cause of strong shielding. Theoretical work on the plasma response is ongoing and new insight can be expected from non-linear and kinetic modelling. Experimentally, a wide-band density fluctuation in the gradient region is found in ELM suppression phases which might play a role for the transport across the edge barrier in the absence of ELMs [9]. Continued experimental work in ASDEX Upgrade will be needed to support and check models for ELM suppression as well as to identify critical parameters for access of and performance with ELM suppression as a basis for extrapolations to fusion reactor plasmas.

This work has been carried out within the framework of the EUROfusion Consortium and has received funding from the Euratom research and training programme 2014-2018 under grant agreement No 633053. The views and opinions expressed herein do not necessarily reflect those of the European Commission.

## References


[1] A Loarte *et al* Nucl. Fusion **54** (2014) 033007

[2] T Evans *et al* Plasma Fusion Res. **7** (2012) 2402046.

[3] W Suttrop *et al*, Plasma Phys. Control. Fus. **59** (2017) 014050

[4] R Nazikian *et al*, IAEA FEC 2016, post-deadline.

[5] W Suttrop *et al*, accepted for Nucl. Fusion, doi = 10.1088/1741-4326/aace93, http://arxiv.org/abs/1804.00933

[6] Y Q Liu *et al*, APS-DPP 2016; Physics of Plasmas **24**, 056111 (2017)

[7] M R Wade *et al*, IAEA FEC 2012, EX/3-1; P B Snyder *et al*, Phys. Plas. **19** (2012) 056115

[8] M E Fenstermacher *et al*, Phys. Plas. **15** (2008) 056122; O Schmitz *et al*, Nucl. Fus. **52** (2012) 043005; M J Lanctot *et al*, Nucl. Fus. **53** (2013) 083019

[9] N Leuthold *et al*, this conference, P1.1109